

Mapping the Dirac point in gated bilayer graphene

A. Deshpande, W. Bao, Z. Zhao, C. N. Lau, and B. J. LeRoy

Citation: [Appl. Phys. Lett.](#) **95**, 243502 (2009); doi: 10.1063/1.3275755

View online: <https://doi.org/10.1063/1.3275755>

View Table of Contents: <http://aip.scitation.org/toc/apl/95/24>

Published by the [American Institute of Physics](#)

Articles you may be interested in

[Band structure mapping of bilayer graphene via quasiparticle scattering](#)

APL Materials **2**, 092503 (2014); 10.1063/1.4890543

[Scanning tunneling spectroscopy of inhomogeneous electronic structure in monolayer and bilayer graphene on SiC](#)

Applied Physics Letters **91**, 122102 (2007); 10.1063/1.2771084

[Electric field effect in ultrathin black phosphorus](#)

Applied Physics Letters **104**, 103106 (2014); 10.1063/1.4868132

[Quantum capacitance devices](#)

Applied Physics Letters **52**, 501 (1988); 10.1063/1.99649

[A transfer technique for high mobility graphene devices on commercially available hexagonal boron nitride](#)

Applied Physics Letters **99**, 232104 (2011); 10.1063/1.3665405

[Valley polarization and intervalley scattering in monolayer MoS₂](#)

Applied Physics Letters **101**, 221907 (2012); 10.1063/1.4768299



Measure Ready
155 Precision I/V Source

- Low-noise excitation for better measurements
- As easy to use as a smartphone

WATCH OUR QUICK-LOOK VIDEO 

Mapping the Dirac point in gated bilayer graphene

A. Deshpande,¹ W. Bao,² Z. Zhao,² C. N. Lau,² and B. J. LeRoy^{1,a)}

¹Department of Physics, University of Arizona, Tucson, Arizona 85721, USA

²Department of Physics, University of California at Riverside, Riverside, California 92521, USA

(Received 15 October 2009; accepted 26 November 2009; published online 17 December 2009)

We have performed low temperature scanning tunneling spectroscopy measurements on exfoliated bilayer graphene on SiO₂. By varying the back gate voltage we observed a linear shift of the Dirac point and an opening of a bandgap due to the perpendicular electric field. In addition to observing a shift in the Dirac point, we also measured its spatial dependence using spatially resolved scanning tunneling spectroscopy. The spatial variation of the Dirac point was not correlated with topographic features and therefore we attribute its shift to random charged impurities. © 2009 American Institute of Physics. [doi:10.1063/1.3275755]

Monolayer graphene (MLG), which is just a single sheet of carbon atoms thick, has unique electronic properties as a consequence of its linear band structure. Stacking one more layer on top of the monolayer gives rise to bilayer graphene (BLG) that is an exciting system with a different set of tunable properties.^{1,2} The bilayer structure is characterized by a quadratic dispersion relation $E = \pm \hbar^2 k^2 / 2m$ with the conduction band and valence bands touching making BLG a zero bandgap semiconductor. When an electric field is applied perpendicular to the plane of carbon atoms, it is possible to open up a bandgap between the conduction band and valence band.^{3–5} Recent experiments with techniques like angle resolved photoemission spectroscopy,⁶ infrared spectroscopy,^{7–9} and transport measurements with a double-gate¹⁰ have confirmed this bandgap opening. These techniques are nonlocal and only provide information about the average properties of the BLG. However, from a device application perspective it is important to get details about how the spatial extent and morphology of the layers affect the electronic properties. Scanning tunneling microscopy (STM) is a powerful tool for this purpose. Previous STM studies have shown that impurities in MLG^{11,12} and phonons¹³ influence the charge-carrier scattering mechanisms in graphene. In this letter, we present scanning tunneling spectroscopy results for BLG on a SiO₂ substrate. These results show the spatial variation of the Dirac point as well as the control of the Dirac point and bandgap due to the application of an electric field from the back gate.

The BLG was prepared using the mechanical exfoliation technique.^{14,15} Degenerately doped Si with 300 nm thick SiO₂ on top was used as a back gate. Bilayer areas were identified using an optical microscope and then Ti/Au electrodes were deposited using a shadow mask technique described elsewhere.¹⁶ The device was then cooled to 4.6 K using an Omicron low temperature STM operating in ultra-high vacuum ($p \leq 10^{-11}$ mbar). Electrochemically etched tungsten tips that exhibited a constant density of states on a Au surface were used for imaging and spectroscopy to avoid unwanted tip effects. Due to the cleaner fabrication procedure, no PMMA is used, it is possible to obtain atomic resolution images over large areas of the BLG without any

additional cleaning procedure unlike in previous STM measurements on exfoliated graphene.^{11–13,17–19}

Figure 1(a) illustrates the concept of bandgap opening for BLG. The measurement set up with STM and back gate connections is shown in Fig. 1(b). The BLG is grounded and voltages are applied to the STM tip and the back gate. As the voltage is increased on the back gate or tip, an electrical field perpendicular to the BLG is established which shifts the Dirac point and opens a bandgap. Figure 1(c) is a 60 nm × 60 nm STM image of the BLG showing modulations due to the underlying SiO₂ substrate as typically seen in MLG samples on a SiO₂ substrate.^{11–13,17–19} The triangular lattice arises due to the presence of two layers that leads to only a single sublattice being observed in the STM images.¹⁸

Figure 2(a) shows a plot of dI/dV as a function of tip and gate voltage. The dI/dV point spectroscopy measurements are performed using standard lockin techniques with an ac modulation of 5 mV rms at 574 Hz. As we sweep

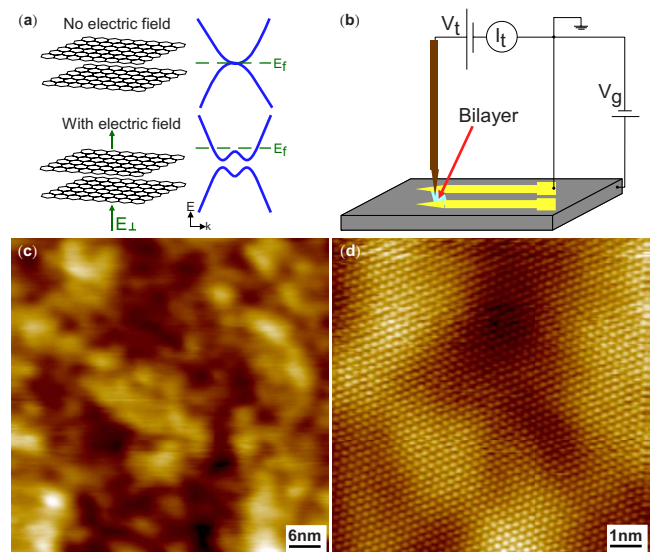


FIG. 1. (Color online) (a) Illustration of bilayer graphene and its band structure with and without a perpendicular electric field. The electric field shifts the Dirac point and opens up a gap. (b) Schematic of mechanically exfoliated bilayer graphene flake showing gold electrodes on a SiO₂ substrate with STM and back gate connections. (c) Constant current STM image of bilayer graphene (0.5 V, 100 pA, 60 nm × 60 nm). (d) Atomic resolution showing the triangular lattice (0.5 V, 100 pA, 10 nm × 10 nm).

^{a)}Electronic mail: leroy@physics.arizona.edu.

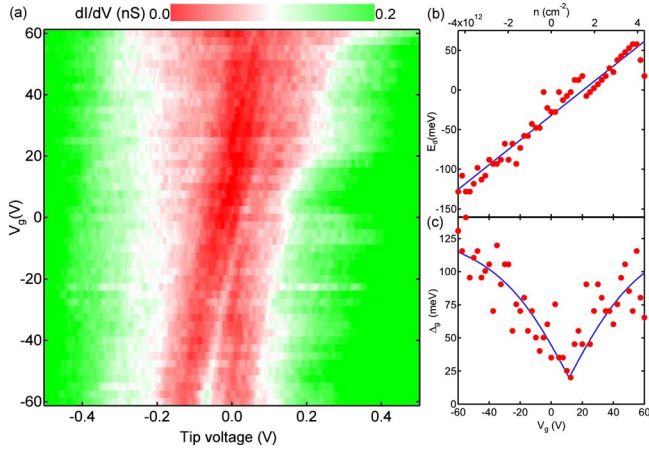


FIG. 2. (Color online) (a) Point spectroscopy measurements of BLG as a function of back gate and tip voltage (energy). The color scale represents the local density of states, dI/dV , with red (dark) areas low and green (light) areas high. The minimum in the density of states corresponds to the Dirac point and it shifts linearly with gate voltage. Similarly, the width of the minimum increases with increasing gate voltage indicating that a bandgap is opening. (b) Position of the Dirac point E_d determined from the dI/dV curves in (a) as a function of the gate voltage V_g (bottom) and induced carrier density n (top). A straight line fit to the data is shown. (c) Bandgap variation with V_g . Dotted line is the fit (see text) to the bandgap variation.

through different gate voltages from -60 to $+60$ V in steps of 2.5 V, two distinct observations can be made. The location of the minimum in the dI/dV curves shifts toward positive tip voltage with increasing gate voltage. Also, the width of the red region which corresponds to low values of dI/dV increases with an increasing gate voltage. In addition, there is an extra peak within the gap (white area visible at negative gate voltages) but further investigation is necessary to attribute it to any of theoretically predicted features like impurities and midgap states.²⁰

The gate voltage induces electrons or holes into BLG and generates an electric field perpendicular to the plane of the bilayer. It leads to an uneven induced charge on each layer and creates an electrostatic potential difference between the two layers that screens the external field and opens a bandgap as predicted by the calculations.³⁻⁵ The red region in Fig. 2(a) shows the bandgap opening with gate voltage and the shift of the Dirac point. From the dI/dV curves we have determined the bandgap at each gate voltage and the energy of the Dirac point based on the position of the minimum in the curve.

A plot of the energy of the Dirac point as a function of the gate voltage (bottom) and induced carrier density (top) is shown in Fig. 2(b). The variation of Dirac point with gate voltage is linear with a slope of 1.56 meV/V. This linear dependence on gate voltage is different from MLG which has a square root dependence due to the linear bandstructure.¹³ The linear dependence is expected for BLG because the bandstructure is quadratic $E = \hbar^2 k^2 / 2m^*$ where m^* is the effective mass of electrons in BLG. For a two-dimensional (2D) system, the electron density is written as $n = k^2 / \pi$. Since the back gate and the BLG act as a parallel plate capacitor, the induced charge on the BLG is given by $n = \frac{\epsilon \epsilon_0 V_g}{et_{ox}}$ where t_{ox} is the thickness of the oxide layer. Putting these equations together gives the shift in energy due to the back gate as $E = \hbar^2 \pi \epsilon \epsilon_0 V_g / 2m^* et_{ox}$. A second effect of the gate voltage is that it leads to an electric field between the

two layers of graphene. Assuming no screening, i.e., each layer carries charge density $n/2$, this field creates a potential difference between the two layers, $V = \frac{edV_g}{2et_{ox}}$ where d is the interlayer separation, 0.335 nm (Ref. 5) and the dielectric constant between the layers is 1. This potential difference reduces the effective voltage between the tip and the BLG. The net effect is that the energy of the Dirac point as observed by the tip shifts as

$$E = \frac{\epsilon V_g}{2et_{ox}} \left(\frac{\hbar^2 \pi \epsilon_0}{m^*} - d \right). \quad (1)$$

Using Eq. (1) we find that the value of effective mass that fits our observed shift of 1.56 meV/V is $0.023m_e$ where m_e is the mass of the electron. Calculations have shown that screening between the layers reduces the potential difference between the layers.^{3,4} Screening reduces the potential between the layers by a factor of 1.6 (Ref. 3) which increases our value of the effective mass to $m^* = 0.030m_e$. This value of the effective mass is slightly lower than tight-binding calculations which give $m^* = 0.033m_e$. However, many body effects can reduce this mass.²¹ Also the electric field due to the tip would tend to lessen the effect of the gate and therefore increase the effective mass needed to fit our data.

Figure 2(c) shows the bandgap as a function of gate voltage V_g and carrier density n . The bandgap has a finite minimum value around a gate voltage of 15 V. This is the voltage needed to have the Dirac point at the Fermi energy and therefore the minimum charge on the BLG. The magnitude of the bandgap is fit using the equation⁴ $\Delta_g = [e^2 V^2 t_{\perp}^2 / (t_{\perp}^2 + e^2 V^2)]^{1/2}$ where V is the potential between the layers and the only free parameter is t_{\perp} the interplane hopping. The best fit occurs for a value of $t_{\perp} = 0.12$ eV which gives an effective mass of $0.017m_e$. Once again, if we take into account the screening between the layers³ we get a value of $t_{\perp} = 0.16$ eV and $m^* = 0.022m_e$.

In the case of MLG the shift of the Dirac point as a function of position leads to the formation of electron and hole puddles that can be seen in density of states measurements.^{11,12,22} To measure the spatial variation of the Dirac point for BLG, we have recorded local density of states (LDOS) maps for large areas of the flake, typically $80 \text{ nm} \times 80 \text{ nm}$. From the individual spectroscopy curves in the LDOS map we have calculated the energy of the Dirac point. This gives the energy of the Dirac point as a function of position in the BLG. Figure 3(a) shows the Dirac point for one such LDOS map. The color scale corresponds to the energy of the Dirac point. A dI/dV curve from an area of positive shift [red square in Fig. 3(a)] is shown in Fig. 3(b). Figure 3(c) shows a dI/dV curve from an area of negative shift [red triangle in Fig. 3(a)]. The energy of the Dirac point is determined by the location of the minimum in these curves. The energy of the Dirac point is not evenly centered around E_f as the average value is at $E_d = 20$ meV. Figure 3(d) shows the topography corresponding to the region in Fig. 3(a). The color scale here corresponds to the height variation of the image. A cross-correlation between Fig. 3(a) and the curvature as calculated from Fig. 3(d) shows no correlation. Hence we claim that the origin of the Dirac point shift, at zero V_g when no charge carriers are induced, lies in the random charged impurities as seen in the case of MLG. The impurity density variation can be calculated from the

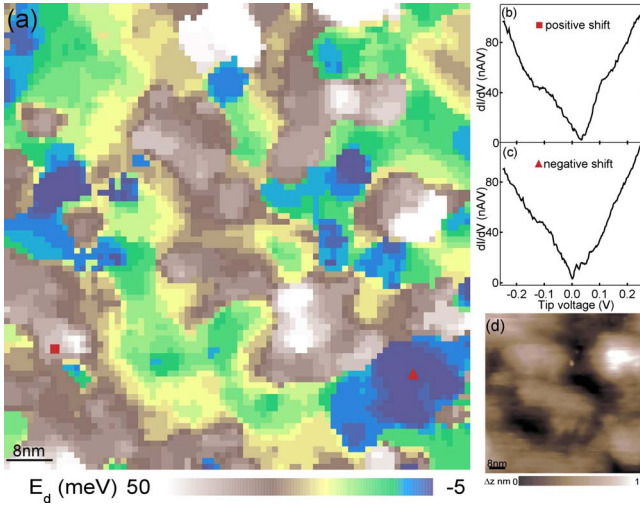


FIG. 3. (Color online) (a) A 2D map (80 nm \times 80 nm) showing the spatial variation of the Dirac point calculated from a dI/dV map of bilayer graphene. The colors correspond to positive and negative shift of the Dirac point. (b) dI/dV curve from the area of positive shift shown in (a) by a filled square. (c) dI/dV curve from the area of negative shift shown in (a) by a filled triangle. (d) Topography of the area shown in (a), (0.5 V, 100 pA, 80 nm \times 80 nm), the color scale shows the height variation of 1 nm.

average measured shift in the Dirac point $\overline{E_d}$ using $\overline{n} = \frac{2m^* \overline{E_d}}{\pi \hbar^2}$ to be $3.8 \times 10^{11} \text{ cm}^{-2}$. These results are consistent with an electrical transport measurement on the BLG which shows the Dirac point shifted slightly away from $V_g = 0$. However, electrical transport measurements give only one number for the Dirac point and do not give any information about its spatial variation.

In conclusion, we have presented scanning tunneling spectroscopy measurements on bilayer graphene on SiO_2 at 4.6 K. Our measurements show that with a back gate it is possible to tune the bandgap and doping in the bilayer. The opening of the bandgap is a promising effect for tailoring the bilayer for electronic applications. In addition, the shift of the Dirac point due to random impurities emphasizes the need to advance the sample preparation methods to ensure minimum impurities.

A.D. and B.J.L. acknowledge the support of the U. S. Army Research Laboratory and the U. S. Army Research

Office under Contract/Grant No. W911NF-09-1-0333. W.B., Z.Z., and C.N.L. acknowledge support under Grants NSF CAREER DMR/0748910, NSF ECCS/0926056, ONR N00014-09-1-0724, and ONR/DMEA H94003-09-2-0901.

- ¹A. K. Geim and K. S. Novoselov, *Nature Mater.* **6**, 183 (2007).
- ²A. H. Castro Neto, F. Guinea, N. M. R. Peres, K. S. Novoselov, and A. K. Geim, *Rev. Mod. Phys.* **81**, 109 (2009).
- ³E. McCann, *Phys. Rev. B* **74**, 161403(R) (2006).
- ⁴E. V. Castro, K. S. Novoselov, S. V. Morozov, N. M. R. Peres, J. M. B. Lopes dos Santos, J. Nilsson, F. Guinea, A. K. Geim, and A. H. Castro Neto, *Phys. Rev. Lett.* **99**, 216802 (2007).
- ⁵H. Min, B. Sahu, S. K. Banerjee, and A. H. MacDonald, *Phys. Rev. B* **75**, 155115 (2007).
- ⁶T. Ohta, A. Bostwick, T. Seyller, K. Horn, and E. Rotenberg, *Science* **313**, 951 (2006).
- ⁷Z. Q. Li, E. A. Henriksen, Z. Jiang, Z. Hao, M. C. Martin, P. Kim, H. L. Stormer, and D. N. Basov, *Nat. Phys.* **4**, 532 (2008).
- ⁸Z. Q. Li, E. A. Henriksen, Z. Hao, M. C. Martin, P. Kim, H. L. Stormer, and D. N. Basov, *Phys. Rev. Lett.* **102**, 037403 (2009).
- ⁹Y. B. Zhang, T. Tang, C. Girit, Z. Hai, M. C. Martin, A. Zettl, M. F. Crommie, Y. Ron Shen, and F. Wang, *Nature (London)* **459**, 820 (2009).
- ¹⁰J. B. Oostinga, H. B. Heersche, X. Liu, A. F. Morpurgo, and L. M. K. Vandersypen, *Nature Mater.* **7**, 151 (2008).
- ¹¹A. Deshpande, W. Bao, F. Miao, C. N. Lau, and B. J. LeRoy, *Phys. Rev. B* **79**, 205411 (2009).
- ¹²Y. Zhang, V. W. Brar, C. Girit, A. Zettl, and M. F. Crommie, *Nat. Phys.* **5**, 722 (2009).
- ¹³Y. Zhang, V. W. Brar, F. Wang, C. Girit, Y. Yayon, M. Panlasigui, A. Zettl, and M. F. Crommie, *Nat. Phys.* **4**, 627 (2008).
- ¹⁴K. S. Novoselov, A. K. Geim, S. V. Morozov, D. Jiang, Y. Zhang, S. V. Dubonos, I. V. Grigorieva, and A. A. Firsov, *Science* **306**, 666 (2004).
- ¹⁵K. S. Novoselov, A. K. Geim, S. V. Morozov, D. Jiang, M. I. Katsnelson, I. V. Grigorieva, S. V. Dubonos, and A. A. Firsov, *Nature (London)* **438**, 197 (2005).
- ¹⁶W. Bao, G. Liu, Z. Zhao, H. Zhang, D. Yan, A. Deshpande, B. J. LeRoy, and C. N. Lau, *Nano Res.* (in press).
- ¹⁷M. J. Ishigami, J. H. Chen, W. G. Cullen, M. S. Fuhrer, and E. D. Williams, *Nano Lett.* **7**, 1643 (2007).
- ¹⁸E. Stolyarova, K. T. Rim, S. Ryu, J. Maultzsch, P. Kim, L. Brus, T. Heinz, M. Hybertsen, and G. W. Flynn, *Proc. Natl. Acad. Sci. U.S.A.* **104**, 9209 (2007).
- ¹⁹V. Geringer, M. Liebmann, T. Echtermeyer, S. Runte, M. Schmidt, R. Ruckamp, M. C. Lemme, and M. Morgenstern, *Phys. Rev. Lett.* **102**, 076102 (2009).
- ²⁰J. Nilsson and A. H. Castro Neto, *Phys. Rev. Lett.* **98**, 126801 (2007).
- ²¹S. V. Kusminskiy, D. K. Campbell, and A. H. Castro Neto, *EPL* **85**, 58005 (2009).
- ²²J. Martin, N. Akerman, G. Ulbricht, T. Lohmann, J. H. Smet, K. Von Klitzing, and A. Yacoby, *Nat. Phys.* **4**, 144 (2008).